Published in final edited form as:
Cell Stem Cell. 2013 December 5; 13(6): 691–705. doi:10.1016/j.stem.2013.11.006.

Human iPSC-based Modeling of Late-Onset Disease via Progerin-induced Aging

Justine D. Miller[1,2,3], **Yosif M. Ganat**[1,2], **Sarah Kishinevsky**[1,2], **Robert L. Bowman**[3,4], **Becky Liu**[1,2], **Edmund Y. Tu**[1,2], **Pankaj Mandal**[6,7], **Elsa Vera**[1,2], **Jae-won Shim**[1,2], **Sonja Kriks**[1,2], **Tony Taldone**[5], **Noemi Fusaki**[9,10], **Mark J. Tomishima**[1,2], **Dimitri Krainc**[8], **Teresa A. Milner**[11,12], **Derrick J. Rossi**[6,7], and **Lorenz Studer**[1,2]

[1]The Center for Stem Cell Biology, Sloan-Kettering Institute for Cancer Research, 1275 York Ave, New York, NY 10065, USA

[2]Developmental Biology Program, Sloan-Kettering Institute for Cancer Research, 1275 York Ave, New York, NY 10065, USA

[3]Gerstner Sloan-Kettering Graduate School, Sloan-Kettering Institute for Cancer Research, 1275 York Ave, New York, NY 10065, USA

[4]Cancer Biology and Genetics Program, Sloan-Kettering Institute for Cancer Research, 1275 York Ave, New York, NY 10065, USA

[5]Molecular Pharmacology & Chemistry, Sloan-Kettering Institute for Cancer Research, 1275 York Ave, New York, NY 10065, USA

[6]Program in Cellular and Molecular Medicine, Boston Children's Hospital, Boston, MA 02115, USA

[7]Department of Stem Cell and Regenerative Biology, Harvard University, Cambridge, MA 02138, USA

Correspondence: Dr. Lorenz Studer, The Center for Stem Cell Biology, Developmental Biology Program, Memorial Sloan-Kettering Cancer Center, 1275 York Ave, Box 256, New York, NY 10065, Phone 212-639-6126, studerl@mskcc.org.

Supplemental Experimental Procedures and any associated references are available in the online version of the paper.

Accession Numbers

The RNA-seq data are available at Gene Expression Omnibus (GEO) (http://www.ncbi.nlm.nih.gov/gds) under the accession number GSE49112.

Author contributions

J.D.M.: conception and study design, reprogramming/maintenance/directed differentiation of iPSCs, cellular/molecular assays, histological analyses, data analysis and interpretation and writing of manuscript. Y.M.G.: mouse transplantation and behavioral analyses. S.K.: mDA neuron-associated assay development and data interpretation. B.L.: western blot analysis and data interpretation. R.L.B.: RNA-seq analysis and data interpretation. E.T.: flow cytometry analysis. P.M.: modified-RNA cloning and technical advice. E.V.: telomere length analysis. J.-W.S., S.K.: mDA differentiation technical advice. T.T.: intracellular dopamine analysis. N.F.: Sendai virus. M.T.: technical advice and data interpretation. D.K.: Derivation of PD-iPSC lines and data interpretation. T.A.M.: electron microscopy and data interpretation. D.J.R.: modified mRNAs and data interpretation. L.S.: conception and study design, data analysis and interpretation and writing of manuscript.

[8]Department of Neurology, Massachusetts General Hospital, Harvard Medical School, Massachusetts General Institute for Neurodegenerative Disease, Charlestown, MA 02129, USA

[9]DNAVEC Corporation, Tsukuba, Ibaraki 300-2611, Japan

[10]Department of Ophthalmology, Keio University School of Medicine, Tokyo, Japan

[11]Brain and Mind Research Institute, Weill Cornell Medical College, 407 East 61st Street, New York, NY 10065, USA

[12]Harold and Margaret Milliken Hatch Laboratory of Neuroendocrinology, The Rockefeller University, 1230 York Ave, New York, NY 10065, USA

Summary

Reprogramming somatic cells to induced pluripotent stem cells (iPSCs), resets their identity back to an embryonic age, and thus presents a significant hurdle for modeling late-onset disorders. In this study, we describe a strategy for inducing aging-related features in human iPSC-derived lineages and apply it to the modeling of Parkinson's disease (PD). Our approach involves expression of progerin, a truncated form of lamin A associated with premature aging. We found that expression of progerin in iPSC-derived fibroblasts and neurons induces multiple aging-related markers and characteristics, including dopamine-specific phenotypes such as neuromelanin accumulation. Induced aging in PD-iPSC-derived dopamine neurons revealed disease phenotypes that require both aging and genetic susceptibility, such as pronounced dendrite degeneration, progressive loss of tyrosine-hydroxylase (TH) expression and enlarged mitochondria or Lewy body-precursor inclusions. Thus, our study suggests that progerin-induced aging can be used to reveal late-onset age-related disease features in hiPSC-based disease models.

INTRODUCTION

Late-onset neurodegenerative disorders such as Parkinson's disease (PD) are becoming a growing burden to society due to the gradual increase in life expectancy. The incidence of PD will likely continue to rise, as it is estimated that by 2050 21.8% of the projected world population (~2 billion people) will be over 60 years of age (Lutz et al., 2008). The use of induced pluripotent stem cell (iPSC) technology where patient-derived skin cells can be reprogrammed back to a pluripotent state and then further differentiated into disease-relevant cell types presents new opportunities for modeling and potentially treating currently intractable human disorders (Bellin et al., 2012). However, there is a concern as to how well iPSC-derived cells can model late-onset diseases where patients do not develop symptoms until later in life, implicating age as a necessary component to disease progression. Several iPSC studies have demonstrated a loss of particular age-associated features during iPSC induction (reviewed in (Freije and López-Otín, 2012; Mahmoudi and Brunet, 2012)). For instance, there is evidence for an increase in telomere length (Agarwal et al., 2010; Marion et al., 2009) and mitochondrial fitness (Prigione et al., 2010; Suhr et al., 2010) and loss of senescence markers (Lapasset et al., 2011) in iPSCs derived from old donors, suggesting that rejuvenation takes place during reprogramming. In addition to the apparent loss of age-associated features in iPSCs, the directed differentiation of human pluripotent stem cells (hPSCs) is known to yield immature, embryonic-like cell types that often require months of

maturation to establish robust functional properties (Liu et al., 2012a; Saha and Jaenisch, 2009). Protracted differentiation is thought to reflect the slow timing of human development. For example, human midbrain dopamine (mDA) neurons, a cell type affected in PD, require months of differentiation to develop mature physiological behaviors and to rescue dopamine deficits in animal models of PD (Isacson and Deacon, 1997; Kriks et al., 2011). These *in vitro* differentiation data argue for a species-specific, intrinsic "clock-like" mechanism that prevents the rapid generation of mature and, aged cells posing a challenge for human iPSC-based modeling of late-onset disorders.

A key problem in addressing global aspects of aging and rejuvenation during cell reprogramming is the identification of markers that reliably measure age in vitro. Candidate age-related cellular markers have been described in fibroblasts derived from Hutchinson-Gilford progeria syndrome (HGPS) patients (Scaffidi and Misteli, 2005, 2006). HGPS is a rare genetic disorder characterized by premature aging of various tissues resulting in early death (Hennekam, 2006). Mutations in *LMNA*, the gene coding for the nuclear envelope protein lamin A, result in the activation of a cryptic splice site which produces a shorter transcript known as progerin. Progerin protein aberrantly accumulates in the nuclear membrane, preventing at least some of the normal scaffolding functions of lamin A, which in turn interferes with multiple processes in the nucleus including chromatin organization, heterochromatin formation, the DNA damage response, cell cycle, gene transcription and telomere maintenance (reviewed in (Dechat et al., 2008)). Interestingly, low levels of progerin are expressed in healthy individuals, and a similar age-associated profile has been observed in fibroblasts from normally aged donors (Scaffidi and Misteli, 2006).

Here we utilize a set of markers that correlates with fibroblast donor age including markers of nuclear morphology and expression of nuclear organization proteins as well as markers of heterochromatin, DNA damage and reactive oxygen species. Such age-associated markers, present in old fibroblasts, were lost during reprogramming and were not reacquired during the subsequent differentiation, indicating that iPSC-derived cells do not maintain a memory of their age. Importantly, we could induce tissue-specific age-associated markers in both iPSC-derived fibroblasts (iPSC-fibroblasts) and iPSC-derived mDA neurons (iPSC-mDA neurons) following short-term progerin exposure. The ability to rapidly induce features associated with cellular age was captured to improve modeling PD *in vitro* and upon transplantation of iPSC-mDA neurons *in vivo*. We observed several age- and disease-related phenotypes not seen in previous iPSC studies including evidence of dendrite degeneration, the formation of age-associated neuromelanin, AKT deregulation, reduction in the number of TH-positive neurons, and ultrastructural evidence of mitochondrial swelling and inclusion bodies. Induced aging presents a novel paradigm for iPSC studies that may be applicable to other cell types and disease pathologies to address the contribution of genetic and age-associated factors in late-onset disorders.

RESULTS

Reprogramming reverts Age-Associated Markers to a "Young" State

In order to validate a marker profile that could be followed during reprogramming and re-differentiation, we compared 12 passage-matched fibroblast populations from apparently

healthy young donors (age 11), middle-aged donors (ages 31-55), old donors (ages 71-96), and prematurely aged HGPS patients (ages 3-14) (Table S1). We observed a significant correlation of donor fibroblast age with age-associated markers (Figure 1A-1C **and** Figure S1A) including markers previously described in HGPS fibroblasts (Scaffidi and Misteli, 2006). Fibroblasts from old donors resembled HGPS fibroblasts supporting previous findings by Misteli and colleagues (Scaffidi and Misteli, 2005, 2006). More specifically, old donor fibroblasts showed nuclear morphology abnormalities (i.e. folding and blebbing), loss of the nuclear lamina-associated protein LAP2α, global loss of the heterochromatin markers tri-methylated H3K9 (H3K9me3) and heterochromatin protein 1 gamma (HP1γ), as well as an increase in DNA damage and mitochondrial reactive oxygen species (mtROS) levels when compared to fibroblasts from younger donors. Importantly, marker expression in old donor fibroblasts was comparable to HGPS fibroblasts despite expressing low levels of progerin, the mutant protein involved in HGPS (Figure S1B). These data suggest that age-associated markers can faithfully stratify young versus old donor fibroblasts.

To address the effects of reprogramming on markers of cellular age, we selected fibroblasts from young (age 11), old (age 82), and HGPS (age 14) donors and transduced them with Sendai vectors expressing Oct4, Sox2, Klf4 and c-Myc (Fusaki et al., 2009) (Figure S1C). The use of the cytoplasmic RNA viruses allowed for the derivation of integration-free iPSCs by 25-40 days post transduction. All iPSC clones demonstrated pluripotent properties and marker expression (Figure S1D-F) and had a normal karyotype (data not shown); and iPSCs derived from HGPS patient fibroblasts maintained the disease mutation (Figure S1G). We next reassessed the age-associated molecular markers shown above to distinguish between young and old fibroblasts. iPSCs were not assessed prior to passage 10 to ensure loss of the exogenous Sendai virus (Figure S1D**).** Following reprogramming, iPSCs which were derived from old donor fibroblasts were indistinguishable from young donor-derived iPSCs with respect to expression of lamin A, LAP2α, H3K9me, and HP1γ (Figure 1D and 1E). Furthermore, all iPSCs displayed minimal levels of DNA damage or mtROS (Figure 1F), suggesting a reset of phenotypic age. However, the age-associated signature could be dependent on progerin expression (Scaffidi and Misteli, 2006) and absence of an age-related phenotype in iPSCs may simply reflect the fact that pluripotent cells do not express A-type lamins including progerin (Constantinescu et al., 2006). Immunocytochemical analysis for all A-type lamin isoforms showed expression restricted to cells undergoing spontaneous differentiation at the periphery of iPSC colonies (Figure 1D, *left column*). HGPS-iPSCs demonstrated a comparable loss of age-associated markers at the pluripotent stage, (Figure 1B-C and 1E-F). However, despite the loss of age-related markers, our data do not rule out the possibility that reprogramming selects for cells with low levels of age-related marker expression (a “young” cell) among the old donor fibroblasts rather than truly re-setting age. Interestingly, clonal growth of primary donor fibroblasts resulted in cultures that reestablished a distribution of age-related markers comparable to the original fibroblast population within two weeks (data not shown). Therefore, it was not possible to obtain fibroblast populations homogeneous in the expression of age-related markers. Nevertheless, regardless of the mechanism, our results demonstrate that iPSCs, independent of donor age or HGPS status, lack expression of age-associated markers.

Age is not induced after Differentiating iPSCs Derived from Old Donors

We next tested whether old donor-derived iPSCs may retain a memory of their donor age that is transiently suppressed at the pluripotent stage. We differentiated iPSCs back into fibroblast-like cells using serum-containing medium (Figure S2A) for 30 days followed by fluorescence-activated cell sorting (FACS) for $CD13^{+}$/$HLA\text{-}ABC^{hi}$ (Papapetrou et al., 2009; Verlinden, 1981) (Figure S2B). The purified cells were expanded for an additional 30 days prior to characterization for the fibroblast marker vimentin and absence of the neural precursor marker nestin (Figure S2C). iPSC-fibroblasts showed expression of lamin A and progerin at levels similar to those observed in primary donor fibroblasts (Figure S2D). However, differentiation did not reestablish the age-associated marker profile in old donor iPSC-fibroblasts (Figure 2A-C) that closely matched the profile of passage-matched young donor iPSC-fibroblasts. These data demonstrate that age-associated markers in primary fibroblasts from aged, apparently healthy donors are reset following reprogramming and are not reestablished upon differentiation into iPSC-fibroblasts. Thus, age is lost after reprogramming, giving rise to phenotypically young iPSC-fibroblasts that may require years of *in vitro* culture to reestablish their age. In contrast, HGPS iPSC-fibroblasts did spontaneously reestablish expression of age-associated markers upon differentiation (Figure 2B and 2C) as reported in iPSC-based models of HGPS (Liu et al., 2011; Zhang et al., 2011), suggesting that cues such as high levels of progerin expression can return iPSC-fibroblasts to an aged-like state.

Acute Progerin Overexpression Reestablishes Age-Related Markers in iPSC-Fibroblasts

We next sought to determine whether progerin overexpression is sufficient to induce age-associated markers in apparently healthy young or old donor iPSC-fibroblasts. Synthetic mRNA (termed modified-RNA) (Kariko et al., 2005; Warren et al., 2010) was used to overexpress either GFP fused to progerin (GFP-progerin) or a nuclear-localized GFP control (nuclear-GFP; Figure S2E), allowing for easy manipulation of the amount and duration of expression. Daily transfection of modified-RNA for three days (Figure 3A) induced progerin expression to levels similar or higher than those in HGPS iPSC-fibroblasts (Figure S2F, *arrows*). Strikingly, overexpression of GFP-progerin but not nuclear-GFP in young and old donor iPSC-fibroblasts induced nuclear morphology abnormalities, loss of LAP2α expression, formation of DNA double strand breaks (γH2AX), loss of heterochromatin markers (H3K9me3 and HP1γ) and increased mtROS **(**Figure 3B-3D). These progerin-induced features were indistinguishable from those observed in primary fibroblasts from aged donors (Figure 1A-1C **and** Figure S1A). Aging in mitotic cells is typically associated with the shortening of telomeres to a critical point when the cell undergoes senescence, reaching Hayflick's limit (Hayflick, 1965). Therefore, we measured telomere lengths using quantitative fluorescence in situ hybridization (Canela et al., 2007) in transfected iPSC-fibroblasts to determine whether progerin can induce telomere shortening. Following progerin overexpression, iPSC-fibroblasts demonstrated a decrease in overall length and an increase in the percentage of short telomeres with progerin overexpression (Figure S2G). This result was further corroborated by an increase in senescence-activated β galactosidase (SA-β-Gal) staining (Figure S2H). All progerin-induced changes in iPSC-fibroblasts were independent of donor age. Our observations indicate that progerin overexpression is

sufficient to rapidly induce phenotypes in iPSC-fibroblasts that phenocopy aspects of normal aging.

Progerin Induces Neuronal Aging Phenotypes in iPSC-mDA Neurons

We next tested whether progerin overexpression also induces age-like phenotypes in a post-mitotic cell type. Therefore, we differentiated young and old donor iPSCs into midbrain dopamine (mDA) neurons, a cell type affected in PD, using our previously established protocol (Kriks et al., 2011) (Figure S3A). Within 13 days, differentiated iPSCs had converted into LMX1A/FOXA2-positive midbrain floorplate precursors, an early stage of mDA neuron development (Figure S3B). Immature mDA neurons at day 32 of differentiation were transiently treated with mitomycin C to eliminate remaining proliferating progenitors (Figure S3C). iPSC-mDA neurons that were matured for an additional six weeks (day 70) continued to express mDA markers such as FOXA2 and tyrosine-hydroxylase (TH) in all iPSC clones independent of donor age (Figure S3D and S3E). Interestingly, iPSC-mDA neurons spontaneously showed evidence of low level nuclear folding concomitant with the onset of endogenous lamin A expression (Figure S3F).

To achieve similar expression levels of progerin in iPSC-mDA neurons as in the iPSC-fibroblasts, we extended modified-RNA exposure to 5 days (Figure 4A), which induced progerin levels exceeding the levels of endogenous lamin A (Figure 4B, *arrows*). Following progerin overexpression GFP-positive cells showed evidence of enhanced nuclear folding and blebbing and accumulation of DNA damage (Figure 4C) and mtROS (Figure 4D). However, in contrast to iPSC-fibroblasts (Figure 3), we did not observe significant changes in LAP2α, H3K9me3 or HP1γ in neurons (Figure 4E). Positive SA-β-Gal staining, a marker of senescence, was also not detected in iPSC-mDA neurons. These data demonstrate both shared and cell type-specific responses of iPSC-fibroblasts and mDA neurons to our *in vitro* aging paradigm.

To further examine cell-type specific responses to progerin exposure, we investigated parameters associated with neuronal aging *in vivo* such as degenerative changes in dendrite branching (Hof and Morrison, 2004). Remarkably, 5 days of progerin exposure in differentiated (day 65) mDA neurons was sufficient to induce a degenerative phenotype resulting in the breakdown of established neurites (Figure 5A). No degeneration was observed in cells transfected with control nuclear GFP mRNA. We next assessed expression of MAP2 which specifically labels dendrites (Bernhardt, 1984). Quantitative analysis showed a marked reduction in average dendrite length following progerin exposure in mDA neurons from both young and old donor iPSCs (Figure 5B). Importantly, the percentages of iPSC-mDA neurons expressing the dopamine neuron markers NURR1 and TH remained unchanged, suggesting that the addition of progerin did not simply induce toxicity (Figure S4A and S4B), in contrast to the treatment with mitochondrial toxins such as CCCP that rapidly induced mDA neuron marker loss (data not shown).

To further characterize the age-like phenotype in iPSC-mDA neurons following progerin overexpression, we performed gene expression analysis by RNA-seq. Principle component analysis confirmed a reset in gene expression following reprogramming and illustrated the similarity between iPSC-mDA neurons from donors of different ages (Figure 5C).

Furthermore, progerin overexpression induced highly similar ($p<2.93 \times 10^{-321}$) changes in young and old donor iPSC-mDA neurons (Figure 5C and Figure S4C). Many of the overlapping progerin-induced expression changes (Figure S4C, and Table S3) have been previously associated with processes involved in neuronal aging, including axon degeneration/regeneration (*TMSB10, TMSB4X, CCDC126, TSNAX, NOSTRIN, LAMC3*), protein misfolding and aggregation (*NEDD8, PSMB3, PPIB, UBC*), oxidative stress (*ENHO, NDUFB6, ATP5L, PRDX4, FTL, ATOX1, TNIP3*), DNA damage (*NOP10, TCEAL7*), cell cycle induction (*PCNA, MIR663A*) and chromatin modification (*PRDM1*) (Figure 5D). Induction of transcripts associated with age-like processes was confirmed by analysis of gene ontology (Figure S4D). Among the differentially expressed transcripts, we also found several uncharacterized genes and non-coding RNAs (Figure 5E) reminiscent of recent observations in the aging rat brain (Wood et al., 2013).

Progerin-induced aging enables modeling of late-onset PD features *in vitro* and *in vivo*

A key motivation for manipulating age in iPSC-neurons is the need for developing faithful models of late-onset neurodegenerative disorders such as PD. Several groups have established iPSC-based disease models of PD. However, those studies reported phenotypes in cell types of uncertain relevance for PD such as neural stem cells (Liu et al., 2012b) or early biochemical phenotypes in mDA neurons without modeling the severe neurodegenerative features of the disease (Cooper et al., 2012; Nguyen et al., 2011; Seibler et al., 2011). We hypothesized that the lack of a neurodegenerative phenotype in those studies may be a result of the age-reset during reprogramming. Similar to PD patients who do not exhibit disease symptoms until later in life, PD iPSC-mDA neurons may be too “young” to mimic the degenerative phase of the disease. Therefore, we tested whether progerin overexpression may reveal disease-associated phenotypes that cannot be currently modeled in PD iPSC studies. We derived mDA neurons from PD-iPSCs with homozygous mutations (Figure S5A) in PINK1 (Q456X) or Parkin (V324A). PINK1 and Parkin are thought to act in a common pathway to promote the autophagic degradation of damaged mitochondria (Dodson and Guo, 2007), in addition to the unique functions of Parkin in the ubiquitin-proteasome pathway (Shimura et al., 2000).

PD-iPSCs differentiated into mDA neurons with similar efficiencies than iPSCs from apparently healthy donors (C1 and C2; Figure S5B and S5C). Furthermore, PD- and control-iPSC-mDA neurons (day 65), transfected with GFP-progerin or nuclear-GFP for 5 days, did not shown changes in NURR1 (Figure 6A) or TH (Figure 6B) expression. We were particularly interested in defining PD-related phenotypes that depend on induced *in vitro* aging and thereby mimic the late-onset nature of the disease. For instance, we observed a significant increase in condensed nuclei that expressed cleaved caspase-3 in PD-versus control-iPSC-mDA neurons (Figure 6C), indicating that PD mutant mDA neurons are more prone to activating a cell death program upon induced aging. GFP-progerin-positive condensed nuclei were not detected until day 4 or day 5 of progerin transfection, suggesting a progressive decline rather than an acute toxicity. Dendrite length in mDA neurons was not significantly affected in PD-versus control-iPSC-mDA neurons under control conditions. However, following progerin overexpression loss of dendrite length was significantly

enhanced in mDA neurons derived from PINK1-Q456X and Parkin-V324A iPSCs versus control-iPSC mDA neurons (Figure 6D and 6E).

It has been suggested that decreased neuronal survival in PD is in part caused by diminished levels of phosphorylated S473 AKT (p-AKT), based on studies in PD models (Malagelada et al., 2008; Tain et al., 2009) and in brain tissues from sporadic PD patients (Timmons et al., 2009). Interestingly, PINK1-Q456X and Parkin-V324A mutant iPSC-mDA neurons showed a significant reduction in p-AKT in response to progerin while C1 and C2 iPSC-mDA neurons showed a slight increase in p-AKT (Figure 6F and 6G). The deregulation of AKT signaling also resulted in the corresponding changes in the phosphorylation of the downstream signaling targets ULK1 and 4EBP1 (Figure 6F and 6G). There was considerable variability in the basal levels of AKT, ULK1 and 4EBP1 across replicate differentiations independent of genotype and treatment (Figure 6F, Figure S5D). However, the progerin-induced reduction in the activation status of AKT signaling components was consistent (independent of basal levels) and mimicked the reported signaling changes in PD.

To further confirm the progerin-induced differences between PD- and control-iPSC-mDA neurons, we reprogrammed additional fibroblasts from a PD patient with a heterozygous R275W Parkin mutation using Sendai virus-based reprogramming. Similar to the progerin-induced phenotype in PINK1-Q456X and Parkin-V324A, progerin overexpression drove increased apoptosis (Figure 6C), enhanced dendrite shortening (Figure 6E) and reduced AKT activation (Figure S5E) in Parkin-R275W iPSC-mDA neurons compared to control-iPSC mDA neurons (C3 and C4).

In order to assess the long-term effects of progerin exposure, mDA neurons derived from PD- and control-iPSCs were transduced with lentiviral vectors expressing *GFP-progerin* or *nuclear-GFP* under the control of the neuron-specific human *synapsin* (*hSyn*) promoter and grafted into the striatum of 6-hydroxydopamine lesioned *NOD-SCID IL2Rgc*-null mice (Figure 7A). *In vitro* analysis of matched aliquots of cells 24-hours after transplantation confirmed expression of NURR1 and TH in GFP-positive cells (Figure S6A). Onset of hSyn-driven transgene expression *in vitro* was detectable 1 day prior to grafting and expression was maintained in cultured cells for at least 90 days (latest time point tested). *In vivo* analysis three months after grafting resulted in a reduction of amphetamine-induced rotation scores in most animals (Figure 7B), indicating mDA neuron survival above the threshold required for behavioral improvement. Interestingly, the subset of animals that did not recover (Figure 7B, *pink symbols*) had received either PINK1- or Parkin-derived neurons expressing progerin. Lack of recovery was surprising considering that survival of only few mDA neurons is required to rescue behavior. To address whether incomplete behavioral recovery in the animals was due to a smaller number of surviving mDA neurons, we performed stereological quantification of the grafts. While graft volume was not significantly affected in progerin-treated versus control groups (data not shown), progerin-expressing mDA neuron grafts showed a dramatic reduction in TH+ cell numbers (Figure 7C and 7D). Strikingly, the reduction in TH+ cells was particularly pronounced in progerin-expressing mDA neuron grafts from PINK1-Q456X and Parkin-V324A iPSCs and minimal in control-iPSC-mDA neuron grafts. Those results mimic the accelerated loss of TH

observed in PD patients, though the mechanism of TH+ cell loss in the current study remains to be determined.

To further assess biomarkers of age and disease status of the iPSC-mDA neurons, we performed ultrastructural analysis of the grafts 6 months after transplantation by transmission electron microscopy (TEM). Initial observations by light microscopy demonstrated a continued, progressive loss of TH immunoreactivity in grafts overexpressing progerin (Figure S6B). Analysis by TEM confirmed the progerin-induced reduction of TH expression in iPSC-mDA neuron dendrites and folded nuclear morphologies (Figure S6C and S6D). To determine the age status of the grafted neurons we focused on the intracellular accumulation of neuromelanin. Neuromelanin is dark colored pigment present in adult mDA neurons but absent in fetal or neonatal stages including iPSC-mDA neurons (Mann and Yates, 1974; Sulzer et al., 2008). In human fetal tissue transplantation studies neuromelanin was detected in grafts 4-14 years after intrastriatal injection, a time course similar to normal development (Loh et al., 2010). In just 6 months, we observed robust accumulation of neuromelanin with lipofuscin deposits selectively in grafts overexpressing progerin (an average of 8 deposits per 55 μm^2 versus 0.5 in control nuclear-GFP expressing grafts, Figure 7E) and regardless of genetic background.

In addition, progerin overexpression revealed genotype-specific effects in PD-iPSC-derived grafts, phenotypes not observed in PD grafts overexpressing nuclear-GFP or in any non-PD control grafts. For instance, signs of neurite degeneration such as the appearance of fibrillar bodies were prominent in PD-derived grafts overexpressing progerin (*asterisks* in Figure 7E and 7G and Figure S6C), indicating a breakdown of microtubules (Jaworski et al., 2011). Furthermore, PINK1-O456X grafts contained cells with enlarged mitochondria, a phenotype much more pronounced in progerin overexpressing cells (area = 0.167 μm^2 compared to 0.0387 μm^2 for PINK1 + nuclear-GFP, p=0.0005; Figure 7F and Figure S6F). In contrast, Parkin mutant grafts showed less dramatic mitochondrial defects (such as abnormal mitochondrial fusion; data not shown) but strikingly, exhibited large multilamellar inclusions (Figure 7G). Multilamellar inclusions have been observed in various neurodegenerative models (Cheng et al., 2011; Phillips et al., 2008) and are considered to be a precursor to the characteristic Lewy bodies found in surviving mDA neurons in brains from Parkinson's patients (Fornai et al., 2004). The presence of these neuronal inclusions suggests decreased function of the ubiquitin-proteasome pathway due to the loss of normal Parkin function. However, the dependence of the phenotype on progerin expression suggests that age-related factors contribute to this dysfunction.

Our *in vivo* results corroborate the *in vitro* data that the age of iPSC-mDA neurons is reset to a "young" state not conducive to modeling late-onset features of PD. In contrast, progerin-induced neuronal aging reveals phenotypes consistent with normal aging as well as disease-associated phenotypes that reflect the synergistic interaction of genotype and age in modeling late-onset degenerative aspects of PD.

DISCUSSION

The ability to measure and manipulate age in cells differentiated from iPSCs represents a fundamental challenge in pluripotent stem cell research that remains unresolved to date. There has been considerable progress in directing cell fate into the various derivatives of all three germ layers; however, there has been no technology to switch the age of a given cell type on demand from embryonic to neonatal, adult or aged status. This remains a major impediment in the field as illustrated by the persistent failure to generate hiPSC-derived adult-like hematopoietic stem cells, fully functional cardiomyocytes, or mature pancreatic islets, and the general inability to derive aged cell types stage-appropriate for modeling late-onset diseases.

The current study represents a first attempt at addressing these challenges. We define a set of cellular markers that correlate with the chronological age of donor fibroblasts, including markers of nuclear organization, heterochromatin, DNA damage and mitochondrial stress. We demonstrate a loss of these age-associated markers upon reprogramming and report that iPSC-derived lineages do not reacquire aging features upon differentiation. We further show that in apparently healthy, non-HGPS cells progerin exposure is sufficient to induce the same set of age-associated markers that define the original old donor fibroblast population prior to iPSC induction. Importantly, we present an induced aging strategy that mimics several aspects of normal aging in iPSC-derived lineages beyond fibroblasts and demonstrate the utility of our approach for modeling late-onset disorders such as PD (Figure S7 **and** Table S2).

A critical requirement for our study was the identification of markers that predict fibroblast donor age and that can be used to monitor cellular age during reprogramming, differentiation and induced aging. In contrast to previous studies (Agarwal et al., 2010; Marion et al., 2009; Prigione et al., 2010; Suhr et al., 2010), it was important to look at a broad set of age-related markers and to compare cellular age in matched cell fates (donor fibroblast versus iPSC-fibroblast). Future studies may include additional candidate markers such as methylation levels at particular CpG sites that have been reported to predict donor age across multiple tissues (Hannum et al., 2013; Koch and Wagner, 2011) or methylation patterns reported to reflect epigenetic memory in iPSCs of donor cell fate (Kim et al., 2010; Polo et al., 2010). It will also be interesting to include additional fibroblast lines covering the age spectrum at even higher resolution and to define whether age-related marker expression increases gradually or occurs as a binary “off/on” switch between young and old age.

One interesting aspect of our approach is the ability to induce cell type-specific responses (Table S2). Progerin-exposure can not only reestablish age in fibroblasts but also phenocopies aspects of normal neuronal aging including the presence of neuromelanin in grafted mDA neurons, global transcriptional changes in mDA neurons after progerin exposure, and progerin-induced *in vitro* dendrite degeneration phenotypes. Furthermore, our results indicate that progerin levels may affect the timing by which age-related phenotypes appear. The use of modified-RNAs rapidly induced very high levels of expression and triggered age-related marker expression within just 3 days in fibroblasts and 5 days in

neurons. In contrast, lentiviral expression under control of a neuronal-specific promoter led to much lower levels of expression that did not trigger an obvious phenotype at 1 month after transplantation (data not shown) but induced robust and progressive phenotypes at 3 and 6 months post grafting. Progerin induced age-related phenotypes occur much more rapidly than during normal aging, making induced aging an attractive yet artificial strategy for modeling late-onset pathology.

It is worth noting that progerin expression using modified-RNAs or expression under a neuron-specific promoter bypasses the differential progerin levels found across various tissues in HGPS patients. Tissue specific expression of A-type lamins is likely the reason why the disease does not affect all organ systems equally (Röber et al., 1989). In particular, the CNS is thought be relatively protected due to the expression of miR-9 which targets lamin A and progerin but not lamin C (Nissan et al., 2012). Therefore, HGPS-iPSC derived neurons are likely not a suitable alternative to the use of progerin synthetic mRNA to trigger *in vitro* neuronal aging.

While progerin exposure may not capture all aspects of normal aging, our study demonstrates that the induced aging strategy triggers an aged-like state suitable for modeling late-onset diseases such as PD in a manner not previously possible in the iPSC field. We observed a robust degenerative phenotype in two genetic PD-iPSC models. In future studies, it will be interesting to mechanistically dissect the separate contribution of genetic and age-related disease susceptibility such as the differences observed in grafted PINK1-versus Parkin mutant iPSC-mDA neurons using isogenic, gene-corrected lines. Similarly, it will be important to perform time course studies to further examine the *progressive* reduction in TH + neurons upon long-term exposure *in vivo* despite our preliminary observations that there are comparable TH+ neuron numbers at early time points after grafting. The ultrastructural inclusions observed in Parkin-derived mDA neurons *in vivo* are compatible with precursor lesions to Lewy body formation. As Lewy bodies are less frequently observed in PD patients with Parkin or PINK1 mutations (Nuytemans et al., 2010), it will be intriguing to test our strategy in additional PD subpopulations such as patients with mutations in α-synuclein or LRRK2 or in sporadic PD. Finally, our technology could be integrated into a drug discovery pipeline aimed at counteracting the increased disease susceptibility of aged cells, a target which cannot be pursued using current PD-iPSC models where the symptom-relevant cells appear “young” and resistant to the degenerative aspect of the disease.

Our work will likely stimulate studies aimed at testing alternative and complementary “induced aging” strategies for modeling late-onset disease. It will also be important to better address the timeline and reversibility of induced aging in iPSC-derived lineages. Furthermore, it will be interesting to test whether expression of progerin at lower levels could facilitate maturation of differentiated iPSC lineages, another key bottleneck in the field. We propose induced aging as a strategy complementary to iPSC technology that may ultimately enable the precise programming of both cell fate and age on demand.

EXPERIMENTAL PROCEDURES

iPSC Derivation and Differentiation

Apparently healthy young donor, old donor and HGPS patient and Parkinson's patient fibroblasts purchased from Coriell were reprogrammed as described (Fusaki et al., 2009) using CytoTune Sendai viruses (Life Technologies) at an MOI of 10. iPSC clones were isolated approximately 4 weeks after transduction and maintained on MEFs with weekly passaging using Dispase (STEMCELL Technologies). For differentiation, iPSCs were harvested using Accutase (Innovative Cell Technology). Fibroblast (Park et al., 2008) and mDA neuron differentiations (Kriks et al., 2011) were performed as previously described.

Modified-RNA Synthesis

Modified-RNA was generated using an *in vitro* transcription (IVT) protocol described previously (Mandal and Rossi, 2013; Warren et al., 2010). Transfections were performed using Lipofectamine RNAiMAX® (Life Technologies) in cell type-specific medium following treatment with an interferon inhibitor (B18R; eBioscience).

Immunocytochemical Analyses

Cells cultures were fixed in 4% paraformaldehyde. A list of antibodies and concentrations is provided in Table S4. Secondary antibodies were species-specific Alexa dye conjugates (Molecular Probes). Additional details for mouse tissue and detailed quantification methods are described in the Supplemental Experimental Procedures.

Flow Cytometry and Mitochondrial ROS Analyses

Cells were dissociated with Accutase and stained with directly conjugated antibodies (BD Biosciences). For Mitochondrial ROS assessment, cells were stained with MitoSOX Red (Life Technologies) at a final concentration of 20 μM in cell culture medium. Cell sorting was performed on a FACSAria (BD Biosciences).

Gene Expression Analysis

Cells were lysed with TriZol (Life Technologies). RNA was extracted using the RNeasy kit (Qiagen) and reverse transcribed using the Superscript kit (Life Technologies) according to the manufacturer's instructions. Quantitative RT–PCR was performed using the Mastercycler RealPlex2 (Eppendorf) platform. For RNA-seq, total RNA was isolated from two independent experiments and processed by the MSKCC Genomic core facility.

Protein Analysis

Cell pellets were lysed with RIPA buffer with 1% sodium dodecyl sulfate (SDS). 20-40 μg samples were further diluted with 4× Laemmli sample buffer, boiled for 5 minutes at 95°C, and loaded onto a NuPAGE 4-12% Bis-Tris precast gel (Life Technologies). PVDF membranes were incubated in primary antibodies overnight (see Table S4 for a list of antibodies used) followed by appropriate HRP-labeled secondary antibodies (Jackson ImmunoResearch).

Xenografts

iPSC-mDA neurons were transplanted into the striatum of lesioned *NOD-SCID IL2Rgc*-null mice (Jackson Laboratory) following *in vitro* transduction with either *hSyn::GFP-progerin* or *hSyn::nuclear-GFP* lentivirus. Immunohistochemistry of the grafts was quantified by stereological analyses. Electron microscopy was performed 6 months following transplantation as described (Milner et al., 2011).

Statistical Analyses

Distributions were compared by statistical analysis of corresponding cumulative distributions using Kolmogorov-Smirnov tests to analyze the difference between different ages or treatments. Bar graphs are plotted as mean ± SEM and represent 3 independent biological replicates except where noted. Two-group comparisons were analyzed using Student t-tests. Multiple group comparisons against a control were analyzed using an ANOVA with Dunnett's test. Prism (version 6.0a, GraphPad) was used for data presentation and analysis.

Supplementary Material

Refer to Web version on PubMed Central for supplementary material.

Acknowledgments

We thank the K. Eggan lab for retroviral-derived control iPSCs, Philip Manos for modified-RNA technical advice, Yvonne Mica and Elizabeth Calder for general technical advice and data interpretation, Andreina Gonzalez, Tracey Van Kempen and Vladimir Mudragel for help in preparing electron microscopy samples, the MSKCC genomics core facility for RNA-seq, MSKCC molecular cytology core facility for histology slices, MSKCC Cytogenetics core facility for karyotyping. D.J.R. is a New York Stem Cell Foundation Robertson Investigator. The work was supported in part by Phil and Marcia Rothblum foundation and by a grant from the Tri-institutional stem cell initiative (Starr foundation) to L.S., grants DA08259 and HL098351 to T.A.M. J.D.M was supported by NSF fellowship.

REFERENCES

Agarwal, S.; Loh, Y-H.; Mcloughlin, EM.; Huang, J.; Park, I-H.; Miller, JD.; Huo, H.; Okuka, M.; Dos Reis, RM.; Loewer, S., et al. Nature. 2010. Telomere elongation in induced pluripotent stem cells from dyskeratosis congenita patients; p. 292-296.

Bellin M, Marchetto MC, Gage FH, Mummery CL. Induced pluripotent stem cells: the new patient? Nat Rev Mol Cell Biol. 2012; 13:713–726. [PubMed: 23034453]

Bernhardt R. Light and electron microscopic studies of the distribution of microtubule-associated protein 2 in rat brain: a difference between dendritic and axonal cytoskeletons. Journal of comparative neurology. 1984; 226:203–221. 1911. [PubMed: 6736300]

Canela A, Vera E, Klatt P, Blasco MA. High-throughput telomere length quantification by FISH and its application to human population studies. Proc Natl Acad Sci U S A. 2007; 104:5300–5305. [PubMed: 17369361]

Cheng HC, Kim SR, Oo TF, Kareva T, Yarygina O, Rzhetskaya M, Wang C, During M, Talloczy Z, Tanaka K, et al. Akt suppresses retrograde degeneration of dopaminergic axons by inhibition of macroautophagy. J Neurosci. 2011; 31:2125–2135. [PubMed: 21307249]

Constantinescu D, Gray HL, Sammak PJ, Schatten GP, Csoka AB. Lamin A/C expression is a marker of mouse and human embryonic stem cell differentiation. Stem Cells. 2006; 24:177–185. [PubMed: 16179429]

Cooper O, Seo H, Andrabi S, Guardia-Laguarta C, Graziotto J, Sundberg M, McLean JR, Carrillo-Reid L, Xie Z, Osborn T, et al. Pharmacological rescue of mitochondrial deficits in iPSC-derived neural cells from patients with familial Parkinson's disease. Science translational medicine. 2012; 4:141–190.

Dechat T, Pfleghaar K, Sengupta K, Shimi T, Shumaker DK, Solimando L, Goldman RD. Nuclear lamins: major factors in the structural organization and function of the nucleus and chromatin. Genes Dev. 2008; 22:832–853. [PubMed: 18381888]

Dodson MW, Guo M. Pink1, Parkin, DJ-1 and mitochondrial dysfunction in Parkinson's disease. Curr Opin Neurobiol. 2007; 17:331–337. [PubMed: 17499497]

Fornai F, Lenzi P, Gesi M, Soldani P, Ferrucci M, Lazzeri G, Capobianco L, Battaglia G, De Blasi A, Nicoletti F, et al. Methamphetamine produces neuronal inclusions in the nigrostriatal system and in PC12 cells. J Neurochem. 2004; 88:114–123. [PubMed: 14675155]

Freije JM, López-Otín C. Reprogramming aging and progeria. Current Opinion in Cell Biology. 2012; 24:757–764. [PubMed: 22959961]

Fusaki N, Ban H, Nishiyama A, Saeki K, Hasegawa M. Efficient induction of transgene-free human pluripotent stem cells using a vector based on Sendai virus, an RNA virus that does not integrate into the host genome. Proc Jpn Acad, Ser B. 2009:348–362. [PubMed: 19838014]

Hannum G, Guinney J, Zhao L, Zhang L, Hughes G, Sadda S, Klotzle B, Bibikova M, Fan JB, Gao Y, et al. Genome-wide methylation profiles reveal quantitative views of human aging rates. Mol Cell. 2013; 49:359–367. [PubMed: 23177740]

Hayflick L. The limited in vitro lifetime of human diploid cell strains. Exp Cell Res. 1965; 37:614–636. [PubMed: 14315085]

Hennekam RCM. Hutchinson-Gilford progeria syndrome: review of the phenotype. American journal of medical genetics Part A. 2006; 140:2603–2624. [PubMed: 16838330]

Hof PR, Morrison JH. The aging brain: morphomolecular senescence of cortical circuits. Trends Neurosci. 2004; 27:607–613. [PubMed: 15374672]

Isacson O, Deacon T. Neural transplantation studies reveal the brain's capacity for continuous reconstruction. Trends Neurosci. 1997; 20:477–482. [PubMed: 9347616]

Jaworski T, Lechat B, Demedts D, Gielis L, Devijver H, Borghgraef P, Duimel H, Verheyen F, Kugler S, Van Leuven F. Dendritic degeneration, neurovascular defects, and inflammation precede neuronal loss in a mouse model for tau-mediated neurodegeneration. Am J Pathol. 2011; 179:2001–2015. [PubMed: 21839061]

Kariko K, Buckstein M, Ni H, Weissman D. Suppression of RNA recognition by Toll-like receptors: the impact of nucleoside modification and the evolutionary origin of RNA. Immunity. 2005; 23:165–175. [PubMed: 16111635]

Kim K, Doi A, Wen B, Ng K, Zhao R, Cahan P, Kim J, Aryee MJ, Ji H, Ehrlich LI, et al. Epigenetic memory in induced pluripotent stem cells. Nature. 2010; 467:285–290. [PubMed: 20644535]

Koch CM, Wagner W. Epigenetic-aging-signature to determine age in different tissues. Aging (Albany NY). 2011; 3:1018–1027. [PubMed: 22067257]

Kriks, S.; Shim, J-W.; Piao, J.; Ganat, YM.; Wakeman, DR.; Xie, Z.; Carrillo-Reid, L.; Auyeung, G.; Antonacci, C.; Buch, A., et al. Nature. 2011. Dopamine neurons derived from human ES cells efficiently engraft in animal models of Parkinson's disease; p. 547-551.

Lapasset L, Milhavet O, Prieur A, Besnard E, Babled A, Aït-Hamou N, Leschik J, Pellestor F, Ramirez J-M, De Vos J, et al. Rejuvenating senescent and centenarian human cells by reprogramming through the pluripotent state. Genes Dev. 2011; 25:2248–2253. [PubMed: 22056670]

Liu G-H, Barkho BZ, Ruiz S, Diep D, Qu J, Yang S-L, Panopoulos AD, Suzuki K, Kurian L, Walsh C, et al. Recapitulation of premature ageing with iPSCs from Hutchinson-Gilford progeria syndrome. Nature. 2011; 472:221–225. [PubMed: 21346760]

Liu G-H, Ding Z, Izpisua Belmonte JC. iPSC technology to study human aging and aging-related disorders. Current Opinion in Cell Biology. 2012a; 24:765–774. [PubMed: 22999273]

Liu G-H, Qu J, Suzuki K, Nivet E, Li M, Montserrat N, Yi F, Xu X, Ruiz S, Zhang W, et al. Progressive degeneration of human neural stem cells caused by pathogenic LRRK2. Nature. 2012b; 491:603–607. [PubMed: 23075850]

Loh Y-H, Hartung O, Li H, Guo C, Sahalie JM, Manos PD, Urbach A, Heffner GC, Grskovic M, Vigneault F, et al. Reprogramming of T cells from human peripheral blood. Cell Stem Cell. 2010; 7:15–19. [PubMed: 20621044]

Lutz W, Sanderson W, Scherbov S. The coming acceleration of global population ageing. Nature. 2008; 451:716–719. [PubMed: 18204438]

Mahmoudi S, Brunet A. Aging and reprogramming: a two-way street. Current Opinion in Cell Biology. 2012; 24:744–756. [PubMed: 23146768]

Malagelada, C.; Jin, ZH.; Greene, LA. Journal of Neuroscience. 2008. RTP801 is induced in Parkinson's disease and mediates neuron death by inhibiting Akt phosphorylation/activation; p. 14363-14371.

Mandal PK, Rossi DJ. Reprogramming human fibroblasts to pluripotency using modified mRNA. Nat Protoc. 2013; 8:568–582. [PubMed: 23429718]

Mann DM, Yates PO. Lipoprotein pigments--their relationship to ageing in the human nervous system. II. The melanin content of pigmented nerve cells. Brain. 1974; 97:489–498. [PubMed: 4423478]

Marion, RM.; Strati, K.; Li, H.; Tejera, A.; Schoeftner, S.; Ortega, S.; Serrano, M.; Blasco, MA. Cell Stem Cell. 2009. Telomeres acquire embryonic stem cell characteristics in induced pluripotent stem cells; p. 141-154.

Milner TA, Waters EM, Robinson DC, Pierce JP. Degenerating processes identified by electron microscopic immunocytochemical methods. Methods Mol Biol. 2011; 793:23–59. [PubMed: 21913092]

Nguyen HN, Byers B, Cord B, Shcheglovitov A, Byrne J, Gujar P, Kee K, Schüle B, Dolmetsch RE, Langston W, et al. LRRK2 mutant iPSC-derived DA neurons demonstrate increased susceptibility to oxidative stress. Cell Stem Cell. 2011; 8:267–280. [PubMed: 21362567]

Nissan X, Blondel S, Navarro C, Maury Y, Denis C, Girard M, Martinat C, De Sandre-Giovannoli A, Levy N, Peschanski M. Unique preservation of neural cells in Hutchinson-Gilford progeria syndrome is due to the expression of the neural-specific miR-9 microRNA. Cell reports. 2012; 2:1–9. [PubMed: 22840390]

Nuytemans K, Theuns J, Cruts M, Van Broeckhoven C. Genetic etiology of Parkinson disease associated with mutations in the SNCA, PARK2, PINK1, PARK7, and LRRK2 genes: a mutation update. Hum Mutat. 2010; 31:763–780. [PubMed: 20506312]

Papapetrou EP, Tomishima MJ, Chambers SM, Mica Y, Reed E, Menon J, Tabar V, Mo Q, Studer L, Sadelain M. Stoichiometric and temporal requirements of Oct4, Sox2, Klf4, and c-Myc expression for efficient human iPSC induction and differentiation. Proceedings of the National Academy of Sciences. 2009; 106:12759–12764.

Park I-H, Zhao R, West JA, Yabuuchi A, Huo H, Ince TA, Lerou PH, Lensch MW, Daley GQ. Reprogramming of human somatic cells to pluripotency with defined factors. Nature. 2008; 451:141–146. [PubMed: 18157115]

Phillips SE, Woodruff EA 3rd, Liang P, Patten M, Broadie K. Neuronal loss of Drosophila NPC1a causes cholesterol aggregation and age-progressive neurodegeneration. J Neurosci. 2008; 28:6569–6582. [PubMed: 18579730]

Polo JM, Liu S, Figueroa ME, Kulalert W, Eminli S, Tan KY, Apostolou E, Stadtfeld M, Li Y, Shioda T, et al. Cell type of origin influences the molecular and functional properties of mouse induced pluripotent stem cells. Nat Biotechnol. 2010; 28:848–855. [PubMed: 20644536]

Prigione A, Fauler B, Lurz R, Lehrach H, Adjaye J. The senescence-related mitochondrial/oxidative stress pathway is repressed in human induced pluripotent stem cells. STEM CELLS. 2010; 28:721–733. [PubMed: 20201066]

Röber RA, Weber K, Osborn M. Differential timing of nuclear lamin A/C expression in the various organs of the mouse embryo and the young animal: a developmental study. Development (Cambridge, England). 1989; 105:365–378.

Saha K, Jaenisch R. Technical Challenges in Using Human Induced Pluripotent Stem Cells to Model Disease. Cell Stem Cell. 2009; 5:584–595. [PubMed: 19951687]

Scaffidi, P.; Misteli, T. Nat Med. 2005. Reversal of the cellular phenotype in the premature aging disease Hutchinson-Gilford progeria syndrome; p. 440-445.

Scaffidi P, Misteli T. Lamin A-dependent nuclear defects in human aging. Science. 2006; 312:1059–1063. [PubMed: 16645051]

Seibler P, Graziotto J, Jeong H, Simunovic F, Klein C, Krainc D. Mitochondrial Parkin recruitment is impaired in neurons derived from mutant PINK1 induced pluripotent stem cells. The Journal of neuroscience: the official journal of the Society for Neuroscience. 2011; 31:5970–5976. [PubMed: 21508222]

Shimura H, Hattori N, Kubo S, Mizuno Y, Asakawa S, Minoshima S, Shimizu N, Iwai K, Chiba T, Tanaka K, et al. Familial Parkinson disease gene product, parkin, is a ubiquitin-protein ligase. Nat Genet. 2000; 25:302–305. [PubMed: 10888878]

Suhr ST, Chang EA, Tjong J, Alcasid N, Perkins GA, Goissis MD, Ellisman MH, Perez GI, Cibelli JB. Mitochondrial rejuvenation after induced pluripotency. PloS one. 2010; 5:e14095. [PubMed: 21124794]

Sulzer D, Mosharov E, Talloczy Z, Zucca FA, Simon JD, Zecca L. Neuronal pigmented autophagic vacuoles: lipofuscin, neuromelanin, and ceroid as macroautophagic responses during aging and disease. J Neurochem. 2008; 106:24–36. [PubMed: 18384642]

Tain, LS.; Mortiboys, H.; Tao, RN.; Ziviani, E.; Bandmann, O.; Whitworth, AJ. Nat Neurosci. 2009. Rapamycin activation of 4E-BP prevents parkinsonian dopaminergic neuron loss; p. 1129-1135.

Timmons, S.; Coakley, MF.; Moloney, AM.; O' Neill, C. Neurosci Lett. 2009. Akt signal transduction dysfunction in Parkinson's disease; p. 30-35.

Verlinden J. Identification of the human fibroblast surface glycoprotein (FSH) as aminopeptidase M. FEBS letters. 1981; 123:287–290. [PubMed: 6112164]

Warren, L.; Manos, PD.; Ahfeldt, T.; Loh, Y-H.; Li, H.; Lau, F.; Ebina, W.; Mandal, PK.; Smith, ZD.; Meissner, A., et al. Cell Stem Cell. 2010. Highly efficient reprogramming to pluripotency and directed differentiation of human cells with synthetic modified mRNA; p. 618-630.

Wood SH, Craig T, Li Y, Merry B, de Magalhaes JP. Whole transcriptome sequencing of the aging rat brain reveals dynamic RNA changes in the dark matter of the genome. Age (Dordr). 2013; 35:763–776. [PubMed: 22555619]

Zhang J, Lian Q, Zhu G, Zhou F, Sui L, Tan C, Mutalif RA, Navasankari R, Zhang Y, Tse H-F, et al. A human iPSC model of Hutchinson Gilford Progeria reveals vascular smooth muscle and mesenchymal stem cell defects. Cell Stem Cell. 2011; 8:31–45. [PubMed: 21185252]

Highlights

- Reprogramming rejuvenates old donor fibroblasts by erasing age-related markers
- Differentiation of old donor iPSCs is not sufficient to trigger memory of age
- Progerin induces age-associated phenotypes in iPSC-derived fibroblasts and neurons
- Progerin reveals late-onset disease phenotypes in iPSC-based models of genetic PD

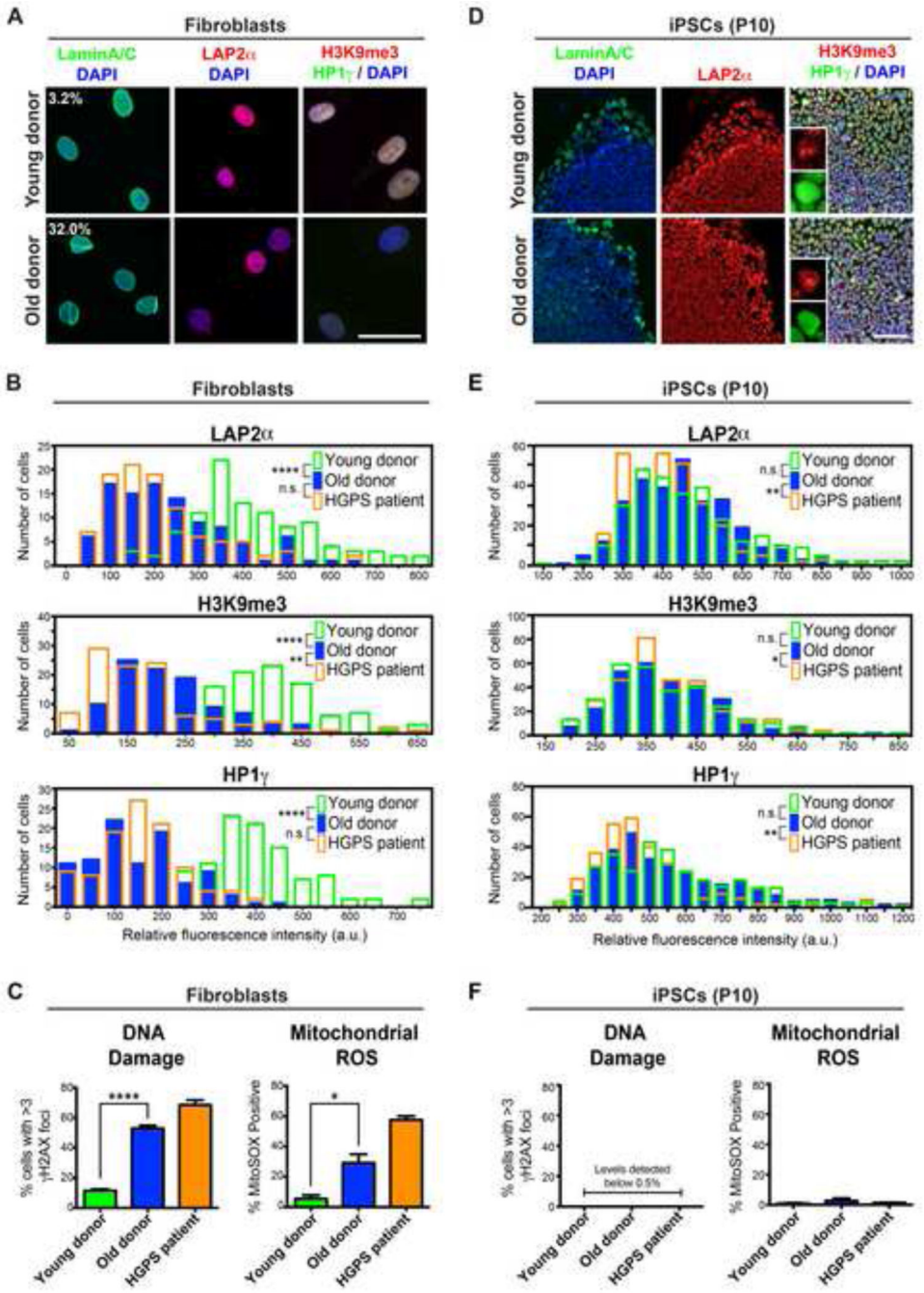

Figure 1. Old Donor Fibroblasts Lose Age-Associated Markers Following Reprogramming to the Pluripotent State

(A) Immunocytochemistry for markers identifying the nuclear lamina (Lamin A/C), a lamina-associated protein (LAP2α) and peripheral heterochromatin (H3K9me3, HP1γ) in young fibroblasts (11-year-old donor) compared to old fibroblasts (82-year-old donor). Percentages indicate the proportion of cells with folded and/or blebbed nuclear morphologies.

(B) Quantification of the markers depicted in (A) demonstrates the ability of the selected age-associated markers to stratify young versus old donor fibroblasts and the similarity of

old donor fibroblasts to HGPS patient fibroblasts. The data are plotted as frequency distributions of relative fluorescence intensity for 100 cells from single fibroblast lines that were passage-matched. a.u., arbitrary units.

(C) Similar to HGPS patient fibroblasts, old donor fibroblasts have higher levels of DNA damage (measured by γH2AX immunocytochemistry) and higher levels of mitochondrial reactive oxygen species (ROS; measured by flow cytometry using the superoxide indicator MitoSOX) than young donor fibroblasts. *n*= 3 independent experiments.

(D) Immunocytochemistry for age-associated markers in passage 10 (P10) iPSCs derived from the young and old donor fibroblasts.

(E) Quantification of staining in (D) indicates loss of age-associated markers during reprogramming of old donor-derived iPSCs (similar to HGPS-derived iPSCs). *n*= 300 cells each (100 cells from 3 independent iPSC clones).

(F) DNA damage and mitochondrial superoxide levels are reset upon reprogramming. *n*= 3 independent clones.

n.s. not significant, **p*<0.05, ***p*<0.01, *****p*<0.0001 according to Kolmogorov-Smirnov tests (B and E) or Student's t tests (C and F). Bar graphs represent mean ± SEM. Scale bars: 50 μm (A), 100 μm (C).

See also Figure S1 and S7 & Tables S1-S2 and S4-S5.

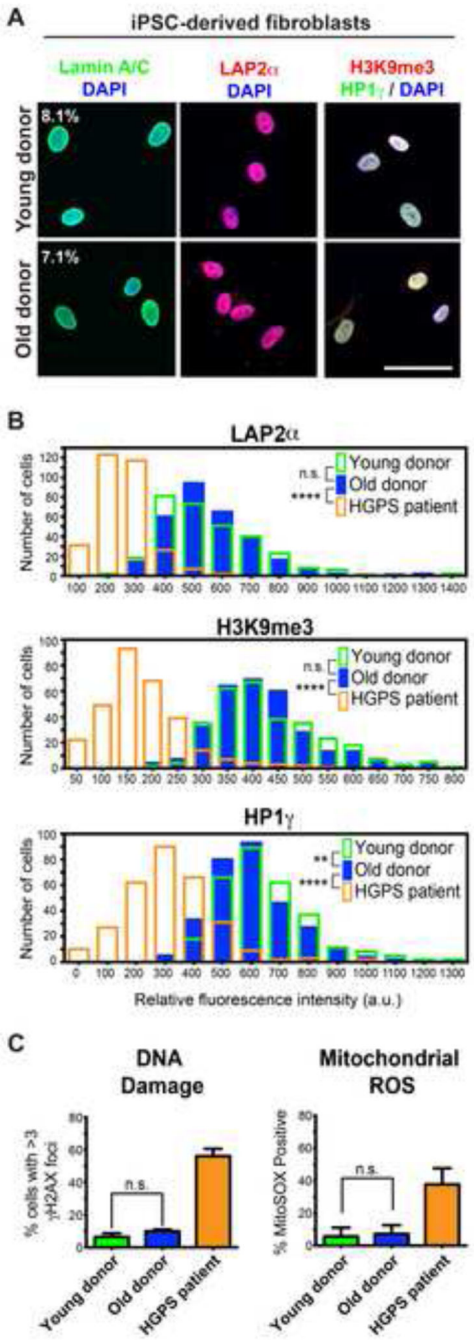

Figure 2. iPSC-Fibroblasts from Old Donors Do Not Regain Age-Associated Markers

(A) Immunocytochemistry for age-associated markers. Percentages indicate the proportion of cells with folded and/or blebbed nuclear morphologies.

(B) Quantification of the markers shown in (A) indicates the high degree of overlap between iPSC-derived fibroblasts (iPSC-fibroblasts) from young and old donors compared to HGPS iPSC-fibroblasts, which reestablish an age-like phenotype.

(C) Analysis of DNA damage (*left*) and mitochondrial superoxide (*right*) further show that iPSC-fibroblasts from old donors have been reset to a “young”-like state.

n.s. not significant, $^{**}p<0.01$, $^{****}p<0.0001$ according to Kolmogorov-Smirnov tests (B) or Student's t tests (C). n= 3 differentiations of independent iPSC clones performed at different times. Bar graphs represent mean ± SEM. Scale bar: 50 μm.
See also Figure S2 and S7 & Tables S2 and S4.

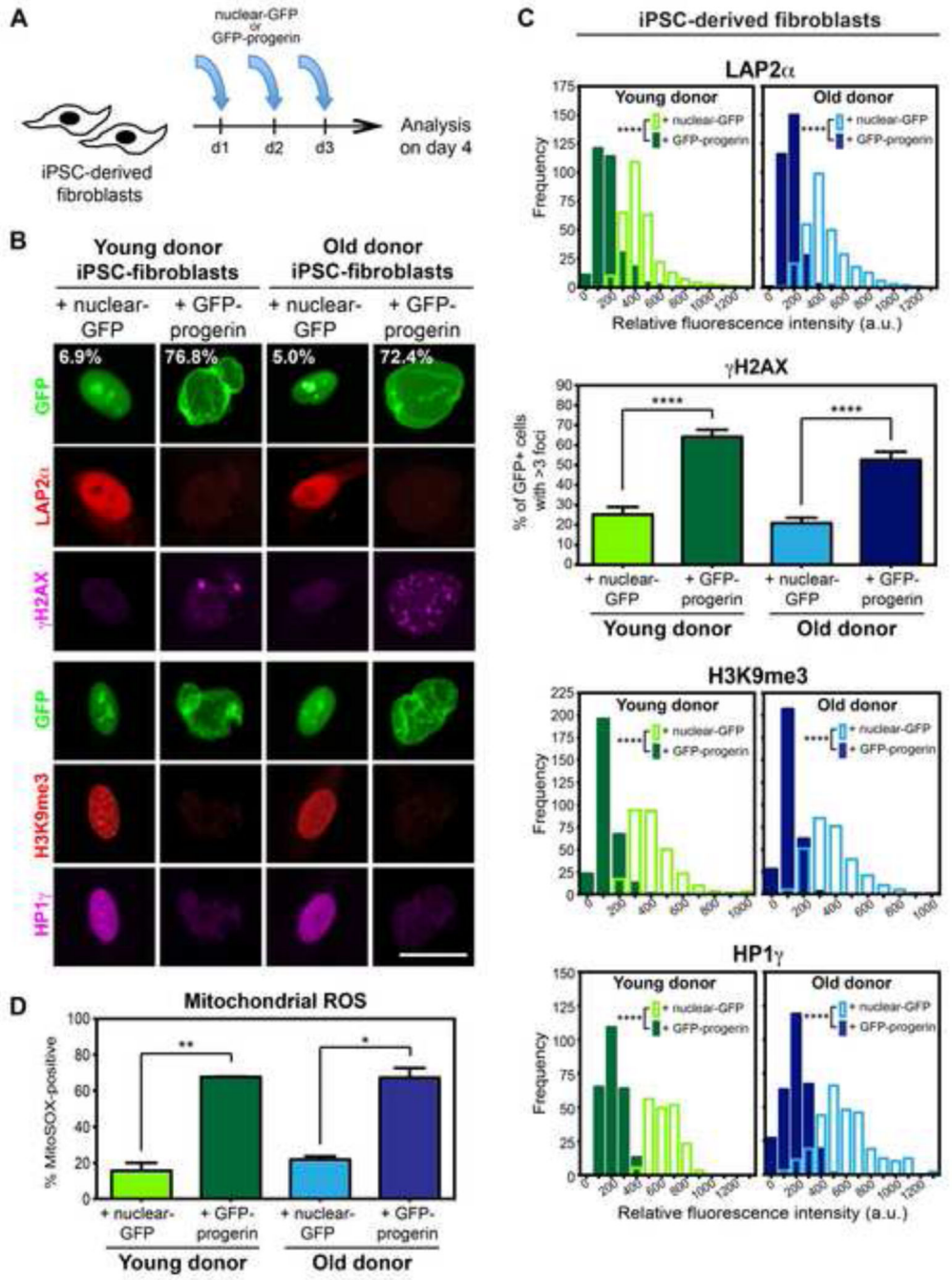

Figure 3. Progerin Overexpression Induces Age-Associated Changes in iPSC-Fibroblasts Regardless of Donor Age

(A) Modified-RNA was transfected into iPSC-fibroblasts on three consecutive days prior to analysis on day 4.

(B) Overexpression of progerin (GFP-progerin) in iPSC-fibroblasts causes changes in nuclear morphology (as seen by GFP), expression of the lamina-associated protein (LAP2α), levels of DNA damage (γH2AX), and chromatin organization (H3K9me3; HP1γ), which were not observed with overexpression of a nuclear-localized GFP control (nuclear-GFP).

Percentages indicate the proportion of cells with folded and/or blebbed nuclear morphologies.

(C) Quantification of data shown in (B). Frequency distribution plots represent the fluorescence intensity of 100 cells from 3 independent RNA transfections of iPSC-fibroblasts derived from independent iPSC clones.

(D) Flow cytometry analysis of the mitochondrial superoxide indicator MitoSOX suggests a dramatic increase in mitochondrial dysfunction with progerin overexpression. n= 3 independent RNA transfections of iPSC-fibroblasts derived from independent iPSC clones. *p<0.05, **p<0.01, ****p<0.0001 according to Kolmogorov-Smirnov tests (LAP2α, H3K9me3, HP1γ) or Student's t-tests (γH2AX, MitoSOX). Bar graphs represent mean ± SEM. Scale bar: 25 μm.

See also Figure S2 and S7 & Tables S2 and S4-S5.

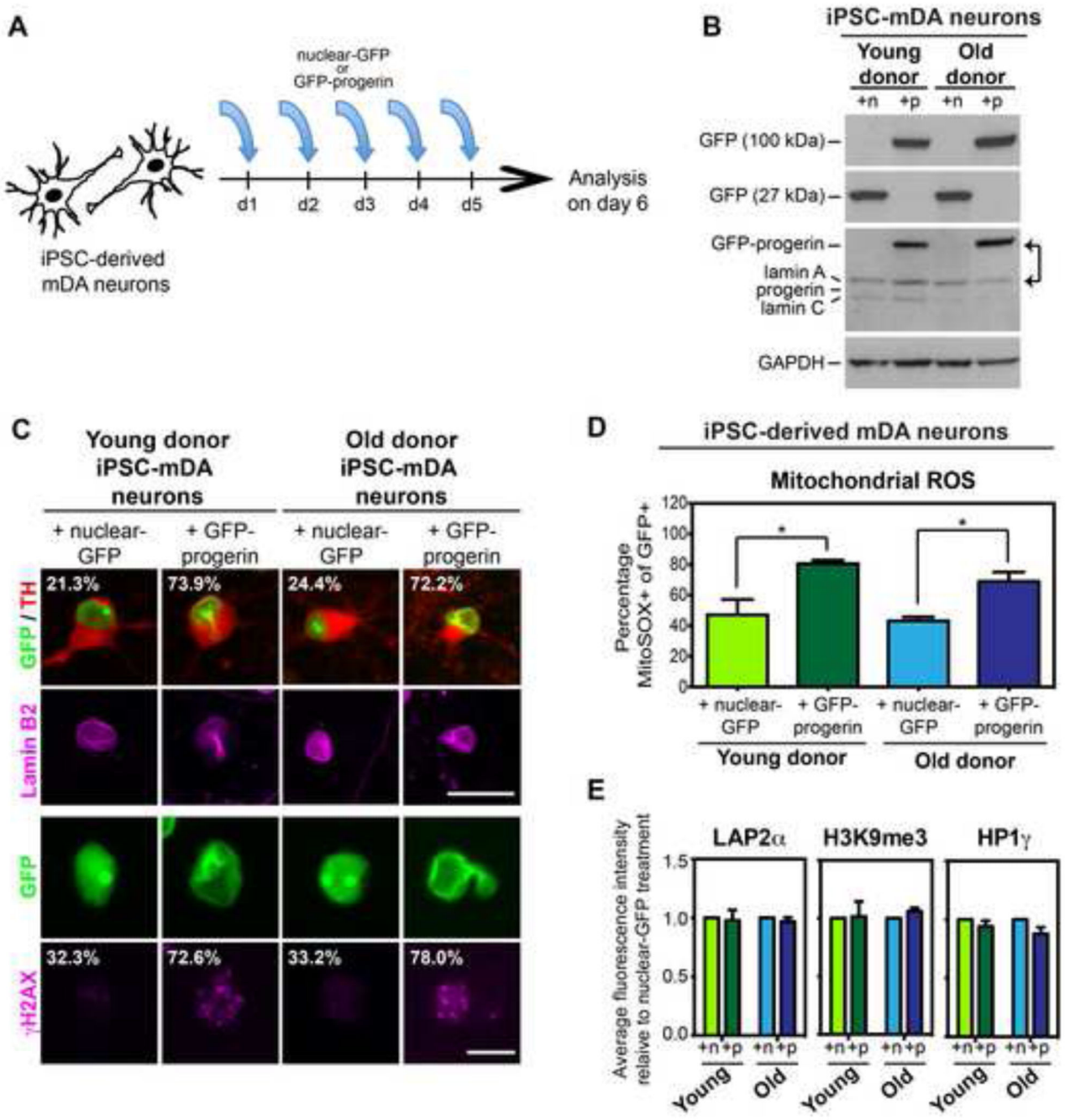

Figure 4. Progerin Overexpression Induces a Subset of the Fibroblast Age-Associated Signature in iPSC-mDA Neurons derived from both Young and Old Donors

(A) Modified-RNA was transfected into iPSC-derived mDA neurons (iPSC-mDA neurons) on five consecutive days prior to analysis on day 6.

(B) Western blot analysis of transgene expression. A GFP band at 100 kDA denotes the GFP-progerin fusion protein while a GFP band at 27 kDA represents the nuclear-GFP transgene. All lamin A isoforms including the transgene were recognized by a single antibody. Note that progerin overexpression levels exceed endogenous lamin A levels

(*arrows*). iPSC-mDA neurons do not appear to express detectable levels of progerin protein endogenously. n, nuclear-GFP; p, GFP-progerin.

(C) Progerin overexpression enhances nuclear folding and blebbing (as seen by lamin B2, pink) and increases DNA damage accumulation (γH2AX) in both young and old donor-derived iPSC-mDA neurons. Percentages indicate the proportion of cells with enhanced nuclear folding and/or blebbing or the proportion of cells with >3 enlarged γH2AX foci.

(D) Flow cytometry analysis of mitochondrial superoxide levels (MitoSOX) demonstrates increased mitochondrial dysfunction with progerin overexpression. *n*= 3 independent RNA transfections of iPSC-mDA neurons derived from independent iPSC clones

(E) Quantification of immunocytochemistry for LAP2α, H3K9me3 and HP1γ shows no difference between iPSC-mDA neurons transfected with GFP-progerin or nuclear-GFP, unlike the phenotype observed in iPSC-fibroblasts (see Figure 3). Fluorescence intensities were normalized to the intensities observed in nuclear-GFP-treated cells.

**p*<0.05 according to Student's t tests (D). Bar graphs represent mean ± SEM. Scale bars: 10 μm (C, *bottom*), 25 μm (C, *top*).

See also Figure S3 and S7 & Tables S2 and S4-S5.

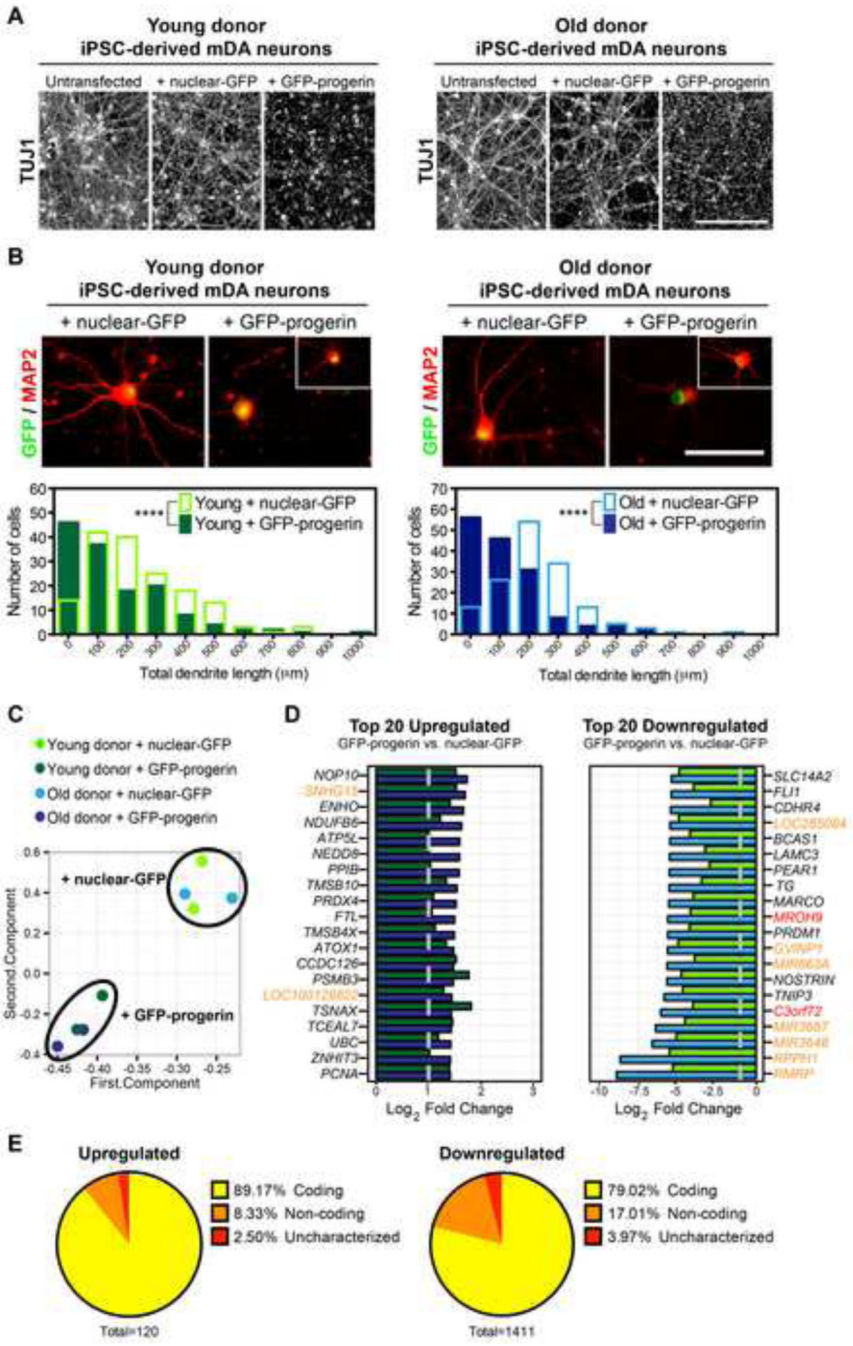

Figure 5. Progerin Overexpression Elicits Features Consistent with Neuronal Aging in iPSC-mDA Neurons

(A) Immunocytochemistry for the pan-neuronal marker TUJ1 shows a loss of the established neuronal network in day 70 iPSC-mDA neurons overexpressing progerin but not iPSC-mDA neurons overexpressing nuclear-GFP.

(B) MAP2 immunocytochemistry reveals reduced intact dendrite lengths following overexpression of progerin in most but not all (*inset*) iPSC-mDA neurons derived from both

young and old donors. Frequency distributions display total dendrite length measurements from 3 independent RNA transfections (50 cells each, non-apoptotic nuclei only).
(C) Principal component analysis of RNA-seq gene expression data further corroborates the reprogramming-induced reset of age that results in the high similarity of iPSC-mDA neurons from both young and old donors. Progerin overexpression induces similar changes in mDA neurons independent of donor age.
(D) The top 20 upregulated (*left*) and downregulated (*right*) genes in progerin-treated compared to control nuclear-GFP-treated young donor (green) and old donor (blue) iPSC-mDA neurons. Genes are ranked according to iPSC-mDA neurons derived from the old donor. Red denotes uncharacterized genes and orange denotes non-coding RNAs. Dotted line indicates the threshold for significance.
(E) Pie charts representing the proportion of the significantly differentially expressed transcripts that are coding, non-coding, or uncharacterized.
****$p<0.0001$ according to Kolmogorov-Smirnov tests. Scale bars: 200 μm (A), 50 μm (B). See also Figure S4 and S7 & Tables S2-S5.

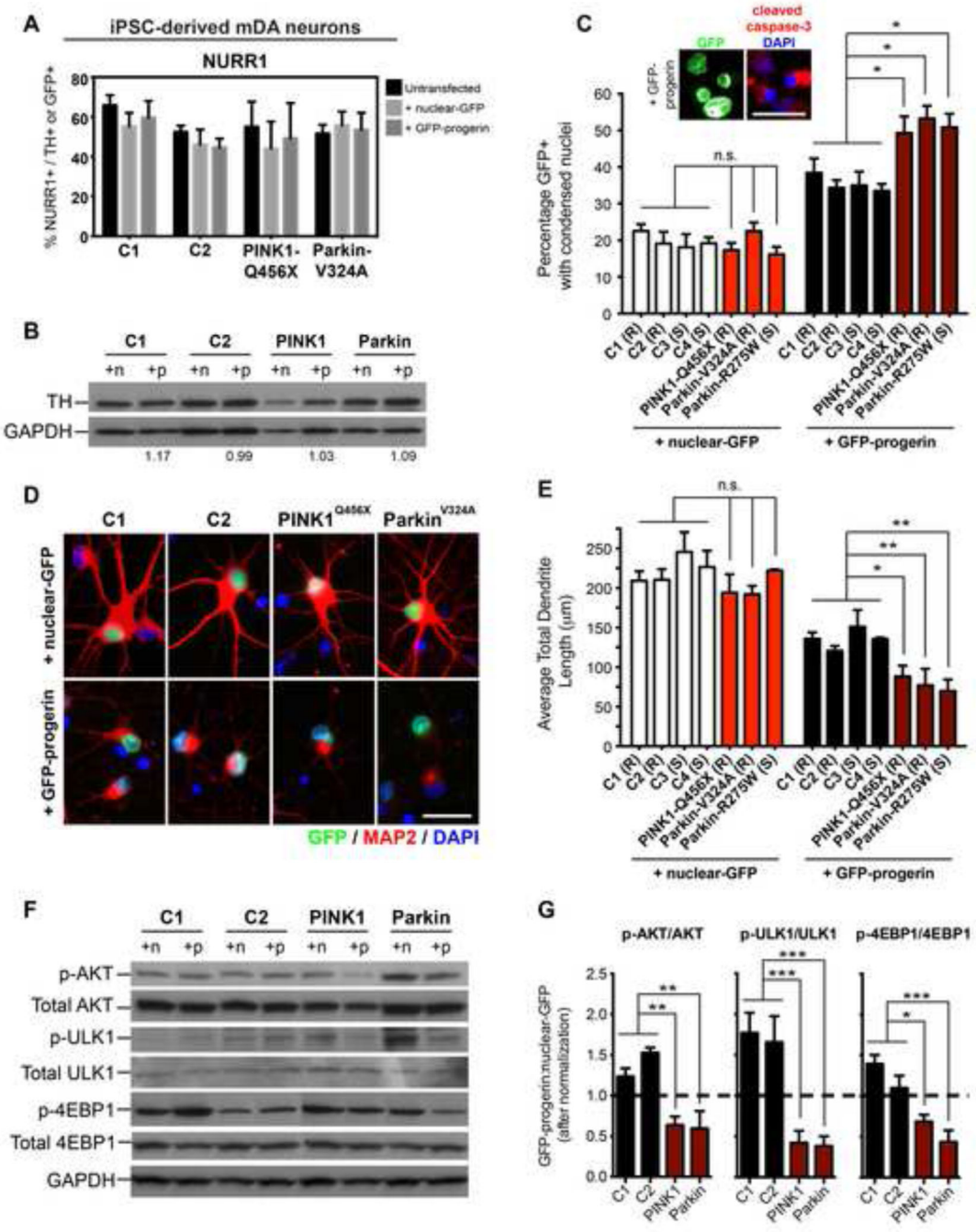

Figure 6. Progerin Overexpression Reveals Disease-Specific Phenotypes *In Vitro* in iPSC-Based Models of Genetic PD

(A and B) Quantification of NURR1+ cells (A) and western blot analysis of TH protein levels (B) do not reveal significant differences with transfection of GFP-progerin modified-RNA. n, nuclear-GFP; p, GFP-progerin. Numbers below the western blot indicate the ratio of GFP-progerin:nuclear-GFP expression of TH normalized to GAPDH.

(C) Analysis of GFP+ cells undergoing cell death following RNA transfection as identified by condensed nuclear morphologies. Images display a representative example of cleaved caspase-3 immunocytochemistry in cells treated with progerin.

(D) Immunocytochemistry for the dendrite marker MAP2.
(E) Quantification of total dendrite lengths per GFP+ neuron shows accelerated dendrite shortening in PD mutant iPSC-mDA neurons compared to apparently healthy controls (C1-4) in response to progerin overexpression.
(F and G) Western blot analysis of AKT pathway signaling (F) demonstrates genotype-specific responses to progerin overexpression. For quantification phospho-specific bands (G) were normalized to total protein before calculating the ratio of the levels expressed following progerin versus nuclear-GFP treatment. Dotted line indicates an equal amount of phospho protein in both treatment conditions. Quantification represents 3 independent cell isolates for each genotype.
*$p<0.05$, ** $p<0.01$, *** $p<0.001$ according to one-way ANOVA with Dunnett's tests ($n= 3$ independent differentiations and modified-RNA transfections in all cases). Bar graphs represent mean ± SEM. n, nuclear-GFP; p, GFP-progerin; C1-4, lines derived from apparently healthy donors; (R), iPSC derived using retroviral factors; (S), iPSC derived using Sendai viral factors. Scale bars: 25 μm.
See also Figure S5 and S7 & Table S2 and Table S4-S5.

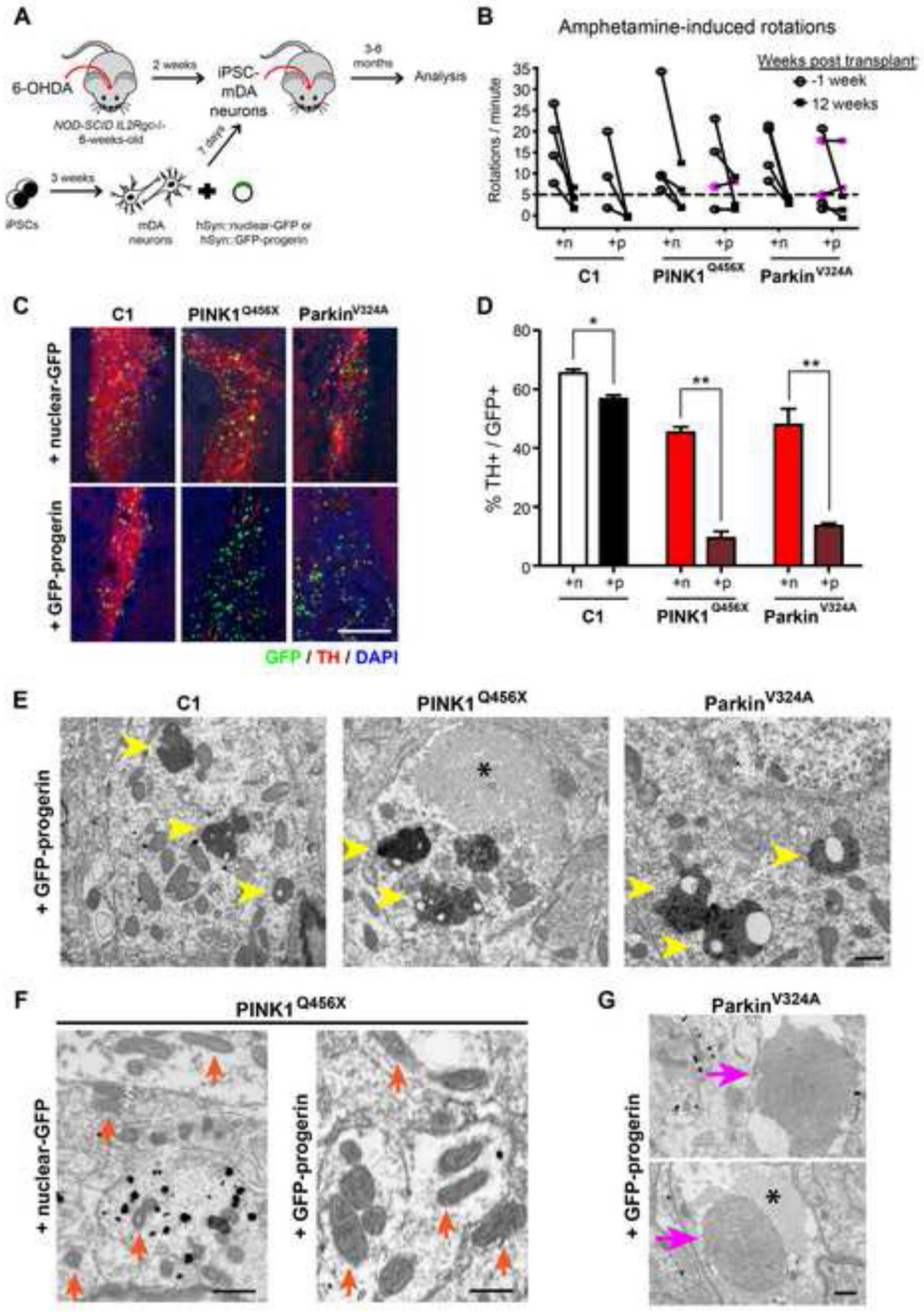

Figure 7. Long-Term Progerin Overexpression *In Vivo* Reveals a Severe Degenerative Phenotype in PD Mutant Cells

(A) Schematic illustration of the transplantation studies into 6-OHDA lesioned Parkinsonian mice.

(B) Rotational behavior analysis of lesioned mice transplanted with control or PD mutant iPSC-mDA neurons expressing *hSyn::nuclear-GFP* or *hSyn::GFP-progerin.* Mice were lesioned and tested for amphetamine-induced rotation behavior twice prior to grafting.

Dotted line indicates threshold for successful lesioning. Pink symbols identify successfully lesioned animals that did not show recovery. *n*= 3-5 animals per treatment group.

(C) Assessment at 3 months post transplant revealed a dramatic loss of TH+ mDA neurons in PD mutants overexpressing progerin.

(D) Quantification of the percentage of GFP+ cells that are TH+. Data are presented as mean ± SEM. *n*= 3 mice per condition.

(E-G) Ultrastructural analysis 6 months after transplantation revealed accumulation of neuromelanin with lipofuscin deposits (E, *yellow arrowheads*) in grafts with progerin overexpression. Strikingly, the PINK1 mutant graft with progerin displayed enlarged mitochondria (F, compare representative mitochondria indicated by *orange arrows* in +nuclear-GFP and +GFP-progerin groups) while the Parkin mutant graft with progerin had large multilamellar bodies (G, *pink arrows*). These phenotypes were not observed in any other treatment groups. Asterisks in (E) and (G) indicate a fibrillar body.

**p*<0.05, ** *p*<0.01 according to Student's t-tests. Bar graph represents mean ± SEM. Scale bars: 200 μm (C), 500 nm (E-G).

See also Figure S6-S7 & Tables S2 and S4-S5.